

## MODELING OF INFILTRATION FRONTS IN HETEROGENEOUS POROUS MEDIA

Insa Neuweiler\*, Cindi Schuetz\*, Alexandros Papafotiou\*, Klaus Mosthaff†,  
Peter Vontobel<sup>+</sup> and Rainer Helmig<sup>†</sup>

\*Leibniz Universitt Hannover Appelstrasse 9a, 30167 Hannover, Germany  
e-mail: neuweiler@hydromech.uni-hannover.de

†University of Stuttgart Pfaffenwaldring 11, 70550 Stuttgart, Germany

<sup>+</sup>Paul Scherrer Institute, 5232 Villigen, Switzerland

**Key words:** Two-phase flow, upscaling, immiscible displacement, memory effects

**Summary.** When modeling immiscible displacement in heterogeneous porous media, such as water infiltration into soil or displacement of water by oil, it is often necessary to describe the fluid distribution in an averaged sense, using upscaled models. Besides the transition zone from high to low displacing fluid content, it is important to capture in an upscaled model fluid exchange with patches of quasi-immobile displaced fluid in the rear of the displacement front. Such patches are also important to capture if macroscopic interfacial area between the fluids need to be quantified. In this contribution we show some examples of displacement experiments, where the occurring of immobile zones in the vicinity of displacement fronts, as well as the transition zones of the displacement fronts are illustrated. We also present an upscaled model, which has a memory term to capture the capillary exchange with immobile zones in a general displacement problem.

### 1 INTRODUCTION

Fast displacement of one fluid by another immiscible one, where the displacement is characterized by the movement of a sharp transition zone between the fluids, plays a major role for many technical applications, such as oil recovery. It is also an important process for subsurface hydrology, when water infiltrates into soil after a heavy rainfall event. When heterogeneous medium structure cannot be modeled in detail, upscaled models are applied to describe the averaged fluid content. Upscaling of two-phase flow cannot be discussed in a general way. Due to the non-linear and complex features of the flow problem, it depends on the flow regime and on the fluid properties, what features are important to capture in an upscaled model.

The upscaled modeling of flow of water and air in the unsaturated zone has been analyzed intensely in a stochastic framework. In most cases the flow problems considered are for capillary equilibrium conditions and describe the slow continuous change of fluid

content, such as during slow drainage in the unsaturated zone. Upscaled models for fast displacement processes, which are characterized by the movement of fronts, have been analyzed mostly in the context of oil displacement problems. Depending on the stability of the homogeneous problem, the models have different features. For neutrally stable displacement an upscaled model has been derived, for example, by [3, 5]. In all papers the averaged spreading of the front leads to a dispersive term in the flow equation, which corresponds to a growth of the width of the transition zone between the fluids with square root of time. For stabilizing fronts, the front width has been analyzed by [6]. Unstable fronts lead in average to a growth of the front width in time. If the macroscopic interfacial area related to the front roughness is considered, it is reasonable to assume that irrespective of the stability criteria the interfacial area relates to the roughness of the front.

The averaged saturation is not necessarily only influenced by the spreading of the front between the fluids. The transition zone of the averaged fluid saturation is also influenced by the occurrence of quasi-immobile patches of displaced fluid. Such patches might come from capillary trapping. It might also be that the fluid is not really trapped but surrounded by the displacing fluid, so that it is slowed down, such that the fluid exchange between stagnant and mobile zones happens on a time scale that is comparable to the typical time scale of the large-scale flow process. In this case the upscaled flow equation has a memory term, which is non-local in time. A model with such memory effects that describes the averaged water content in soil based on the Richards equation has been derived by [4].

In this contribution we derive an upscaled model for fast infiltration, where pressure gradients in both phases need to be considered. The model captures stagnant zones. We will in the next section motivate the capturing of stagnant zones in immiscible displacement problems with experimental findings. In the last section we will demonstrate the homogenization of an immiscible displacement model with stagnant zones, which leads to a memory term in the upscaled flow equation.

## 2 IMMISCIBLE DISPLACEMENT EXPERIMENTS AND EXCHANGE WITH STAGNANT ZONES

To motivate the capturing of stagnant zones in upscaled models for immiscible displacement, two experiments on displacement fronts are shown in the following section. In both cases there is additionally to the main flow capillary exchange to stagnant areas.

### 2.1 Displacement front for drainage

The following experiments is taken from [1]. In these experiments, water was displaced by oil in a glass box of 40 x 60 x 1.2 cm, filled with glass beads. Although this is a drainage instead of an imbibition, similar phenomena would also be expected for imbibition. Two types of glass beads of different sizes were used and the packing was arranged with a

background - inclusion pattern. The inclusions have a smaller entry pressure for the non-wetting (oil) phase and are therefore invaded preferentially. The details of the experiments can be found in [1]. Figure 1 shows the movement of the displacement front. In the middle of the box one patch of background material is surrounded (in an open structure) by coarse inclusion material. As the non-wetting fluid invades the coarse material, the displaced fluid in the patch is not well connected to the rest of the background material, forming a quasi-stagnant zone. For this experiment it can be observed from Figure 1 that the time needed to fill the quasi-stagnant patch is comparable to the time needed by the displacement front to reach the bottom of the sand box.

The front roughness may be modeled with an upscaled model for stabilizing or neutrally stable displacement. Such a model would, however, not capture the exchange with the stagnant zone behind the front.

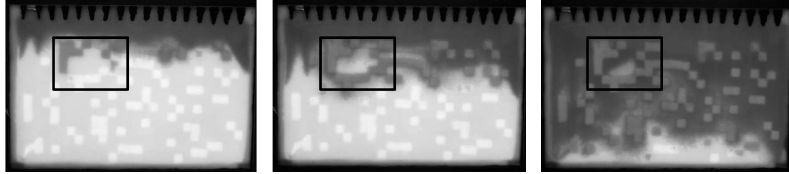


Figure 1: Displacement of water by NAPL at three different times.

## 2.2 Unstable infiltration front

The following example shows an experiment of unstable water infiltration into dry coarse sand with inclusions of fine sand (preferentially invaded by water) in a cylindrical column with a diameter of 10 cm and a height of 15 cm. The coarse sand had a grain size distribution of 0.7-1.2 mm. The top of the column was covered with fine sand in order to have an even infiltration plane. The water content was measured using neutron radiography at the NEUTRA station at the Paul Scherrer Institute in Villigen, Switzerland. The column was placed in-between the neutron beam-line and a scintillator screen, where the intensity of neutrons was measured. The neutron intensity can (neglecting scattering effects) be described by Lambert Beers law

$$I = I_0 \exp \left( - \sum_i \sigma_i d_i \right). \quad (1)$$

$I$  is the intensity measured at the scintillator screen,  $\sigma_i$  is the absorption coefficient for material  $i$  and  $d_i$  is the thickness of the material  $i$  that has been passed by the neutron beam. In our case the relevant materials are quartz (sand), water, which is indicated by  $w$  and aluminum of the column walls. The absorption by air is neglected. By measuring

the intensity of the beam after passing the dry column,  $I_{\text{dry}}$ , the water thickness over the depth of the column during the infiltration process can be determined as

$$\ln\left(\frac{I_{\text{dry}}}{I}\right) = \sigma_w d_w. \quad (2)$$

As the column had a thickness of 10 cm, deuterium was used in the experiments instead of water, which has a smaller absorption coefficient than water. The absorption coefficient  $\sigma_w$  was calibrated by comparing the water mass in the column calculated with the water thickness  $d_w$  to mass measurements with a balance. From the water thickness  $d_w$  and the column thickness the depth averaged water content  $\Theta$  can be calculated.

Figure 2 shows on the left side the water thickness in cm after breakthrough. The inclusion cells are drawn into the figure. It can be observed that the infiltration front is unstable and that water infiltrates preferably into the inclusions and in the compacted zones, which were generated when the inclusions were packed. These zones do not stabilize the front. On the right hand side of Figure 2 the shape of the water front is shown, by adding the segmented picture of the water content (which has a value of one for water content larger than zero and zero otherwise) at four time steps.

The storage cells and compacted zones act as sources for a slight lateral spreading, which takes place by capillary exchange flow between dry sand and the wet sand of the inclusions.

The roughness of the infiltration front may be modeled by an upscaled model for the unstable flow. Such a model would, however, not capture the lateral exchange with the dry zones.

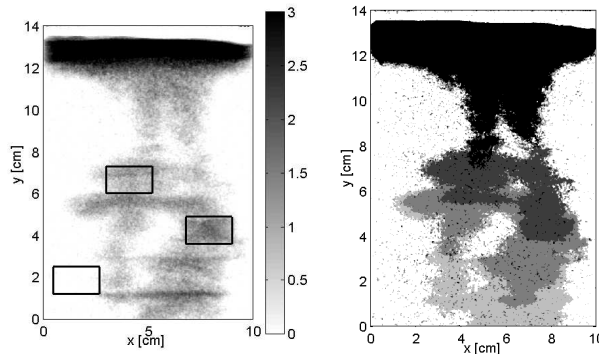


Figure 2: Displacement of air by water. Left: water thickness  $d_w$  [cm] after breakthrough. Right: Water front at four different time steps. Darker shades indicate later times.

### 2.3 Quasi-stagnant zones

If the fluid content in the experiments shown above would be modeled by an upscaled model that describes the horizontally averaged fluid content, the front might be captured

by a term that causes a spreading with time for the unstable case or with square root of time for the first example. However, the capillary flow into the quasi-stagnant zones would not be captured by such a model. In the following we will derive an upscaled model that contains the front roughness and additionally captures the stagnant zones using homogenization theory.

### 3 HOMOGENIZED DISPLACEMENT MODEL WITH EXCHANGE WITH STAGNANT ZONES

#### 3.1 Flow model

We proceed from the assumption that both the displacing and the displaced fluids are incompressible and we neglect hysteretic parameter relations and dynamic effects. The Darcy velocity  $\vec{q}_i$  of each fluid  $i$  is described as

$$\vec{q}_i = -\frac{K_0}{\mu_i} k_r(S_i) \left( \vec{\nabla} P_i + \rho_i g \vec{e}_z \right), \quad (3)$$

where  $K_0$  is the intrinsic permeability of the medium,  $P_i$  is the pressure of phase  $i$ ,  $\mu_i$  is its viscosity and  $\rho_i$  its density.  $g$  is the gravity constant and  $k_r$  is the relative permeability of phase  $i$ . The pressure difference between the phases, the capillary pressure  $P_c$ , is assumed to be a unique function of fluid saturation

$$P_{nw} - P_w = P_c(S). \quad (4)$$

The phases sum up to one,  $S_n + S_{nw} = 1$ , where  $nw$  indicates non-wetting and  $w$  indicates wetting fluid. A continuity equation for each phase can be formulated. By changing the variable phase pressure to the total flow velocity  $\vec{q}_{\text{total}} = \vec{q}_w + \vec{q}_{nw}$ , the continuity equation for the displacing fluid can be written as

$$\frac{\partial S_i}{\partial t} + \vec{q}_{\text{total}} \cdot \vec{\nabla} f_i(S) - \vec{\nabla} \cdot \frac{K_0}{\mu_j} \Lambda(S) \vec{\nabla} P_c(S) - \vec{\nabla} \cdot \frac{K_0 g \Delta \rho}{\mu_j} \Lambda(S) \vec{e}_z = 0. \quad (5)$$

$\Delta \rho$  is the difference between the densities of both fluids.  $f(S)$  is the fractional flow function  $f_i = k_{ri}/(k_{ri} + \mu_i/\mu_j k_{rj})$  and  $\Lambda(S) = k_{rj} f_i(S)$ . The Darcy flow velocity of the displaced fluid can be expressed with these variables as

$$\vec{q}_i = \vec{q}_{\text{total}} f_i(S) - \frac{K_0}{\mu_j} \Lambda(S) \vec{\nabla} P_c(S) - \frac{K_0 g \Delta \rho}{\mu_j} \Lambda(S) \vec{e}_z \quad (6)$$

The index will be dropped in the following.

The continuity equation (5) for the displaced fluid can be written in dimensionless form

$$N_f \frac{\partial S}{\partial t} + N_{\text{Ca}}^{-1} \vec{q}_{\text{total}} \cdot \vec{\nabla} f(S) - \vec{\nabla} \cdot \Lambda(S) \vec{\nabla} P_c(S) - N_g \vec{\nabla} \cdot \Lambda(S) \vec{e}_z = 0. \quad (7)$$

All variables are here considered dimensionless. The dimensionless numbers are chosen as  $N_f = (L^2\mu)/(TK_0P_e)$ ,  $N_{Ca} = (K_0P_e)/(QL\mu)$  and  $N_g = (\Delta\rho gL)/P_e$ .  $L$  is a typical length,  $T$  a typical time,  $P_e$  is a typical pressure difference related to the capillary pressure and  $Q$  is the mean total flow velocity.

### 3.2 Length scale expansion and dimensionless numbers

We will in the following assume that the porous medium is homogeneous with a clearly defined unit cell, as usually assumed in homogenization theory. The details are explained for example in [2]. The macroscopic length scale,  $L$ , is the typical length scale of the system. The typical length scale for the unit cell,  $\ell$ , is clearly distinct from  $L$ . This provides an expansion parameter  $\varepsilon = \ell/L$ . It is assumed that the space variable made dimensionless with the small length scale, which is denoted as  $\hat{Y}$  and independent of the variable made dimensionless with the large length scale  $L$ , which is denoted as  $\hat{X}$ .

We assume now that the porous medium consists of two materials, the material where the main flow takes place, which is indicated with  $\Omega_1$  and the stagnant inclusions, indicated with  $\Omega_2$ . That  $\Omega_2$  is a stagnant zone implies that the total flow velocity in the stagnant zones is of much lower and thus of higher order in the expansion parameter  $\varepsilon$  than that in the background material. Typical scaling of the dimensionless numbers for such a scenario could be

$$\Omega_1 : N_{f1} \propto \varepsilon^{-1}, N_{Ca1}^{-1} \propto \varepsilon^{-1}, N_{g1} \propto \varepsilon^0, \quad \Omega_2 : N_{f2} \propto \varepsilon^{-2}, N_{Ca2}^{-1} \propto \varepsilon^0, N_{g2} \propto \varepsilon^0. \quad (8)$$

The continuity equation (7) for each material (1 and 2) is fulfilled separately. At the material boundaries between  $\Omega_1$  and  $\Omega_2$ ,  $\Gamma_{12}$ , the capillary pressure has to be continuous.

$$P_{c1}|_{\Gamma_{12}} = P_{c2}|_{\Gamma_{12}} \quad (9)$$

Also, the total flow velocity has to be continuous at the interface

$$\vec{q}_{\text{total}1} \cdot \vec{n}|_{\Gamma_{12}} = \vec{q}_{\text{total}2} \cdot \vec{n}|_{\Gamma_{12}} \quad (10)$$

### 3.3 Homogenized model

The saturation in each domain is expanded in terms of the scaling parameter  $S_i = S_i^{(0)} + \varepsilon S_i^{(1)} + \varepsilon^2 S_i^{(2)} + \dots$ . The constitutive relations  $f(S)$ ,  $\Lambda(S)$  and  $P_c(S)$  are expanded as Taylor expansions around  $S_i^{(0)}$ . All orders  $S_i^{(n)}$  are  $\hat{Y}$ -periodic (but not necessarily continuous). We assume now that as  $\varepsilon$  is very small, the continuity equation has to be fulfilled for all terms of one order  $\varepsilon^n$  independently of the other orders. The gradient is split according to  $\vec{\nabla}/L \rightarrow \vec{\nabla}_{\hat{X}} + 1/\varepsilon \vec{\nabla}_{\hat{Y}}$ . For more details of the approach see, for example, [2].

We consider first only the continuity equation in  $\Omega_1$ . The highest order equation is of order  $\varepsilon^{-2}$  and reads

$$N_{Ca1}^{-1} \vec{q}_{\text{total}1} \cdot \vec{\nabla}_{\hat{Y}} f_1^{(0)} + \vec{\nabla}_{\hat{Y}} \cdot \Lambda_1^{(0)} \vec{\nabla}_{\hat{Y}} P_{c1}^{(0)} = 0 \quad (11)$$

with the highest order of the flux condition (10)

$$\left[ N_{\text{Ca}1}^{-1} \vec{q}_{\text{total}1} f_1^{(0)} - \Lambda_1^{(0)} \vec{\nabla}_{\hat{Y}} P_{c1}^{(0)} \right] \cdot \vec{n} \Big|_{\Gamma_{12}} = 0. \quad (12)$$

This is solved by  $S_1^{(0)} = S_1^{(0)}(\hat{X}, t)$ . This means that the saturation in  $\Omega_1$  is constant on the small length scale and varies only on the large length scale  $\hat{X}$ . The inclusions are seen as impermeable obstacles.

The terms of the next highest order  $\varepsilon^{-1}$  read

$$N_{f1} \frac{\partial}{\partial t} S_1^{(0)} + N_{\text{Ca}1}^{-1} \vec{q}_{\text{total}1} \cdot (\vec{\nabla}_{\hat{X}} f_1^{(0)} + \vec{\nabla}_{\hat{Y}} f_1^{(1)}) - \vec{\nabla}_{\hat{Y}} \cdot (\Lambda_1^{(0)} \vec{\nabla}_{\hat{X}} P_{c1}^{(0)} + \Lambda_1^{(0)} \vec{\nabla}_{\hat{Y}} P_{c1}^{(1)} + N_{g1} \Lambda_1^{(0)} \vec{e}_z) = 0 \quad (13)$$

with the next highest order of the flux condition (10)

$$\left[ N_{\text{Ca}1}^{-1} \vec{q}_{\text{total}1} f_1^{(1)} - \Lambda_1^{(0)} \vec{\nabla}_{\hat{X}} P_{c1}^{(0)} - \Lambda_1^{(0)} \vec{\nabla}_{\hat{Y}} P_{c1}^{(1)} - N_{g1} \Lambda_1^{(0)} \vec{e}_z \right] \cdot \vec{n} \Big|_{\Gamma_{12}} = 0. \quad (14)$$

Averaging the continuity equation spatially averaged over the domain  $\Omega_1$  of the unit cell yields the highest order of the homogenized flow problem

$$N_{f1} \frac{\partial}{\partial t} S_1^{(0)} + N_{\text{Ca}1}^{-1} \langle \vec{q}_{\text{total}1} \rangle_{\Omega_1} \cdot \vec{\nabla}_{\hat{X}} f_1^{(0)} = 0. \quad (15)$$

By subtracting the averaged equation from the non-averaged equation, we obtain an equation for  $S_1^{(1)}$ , denoting  $\vec{q}_{\text{total}1} - \langle \vec{q}_{\text{total}1} \rangle = \tilde{q}_{\text{total}1}$  and taking into account that  $S^{(0)} = S^{(0)}(\hat{X}, t)$ ,

$$N_{\text{Ca}1}^{-1} \tilde{q}_{\text{total}1}(\hat{Y}) \cdot \vec{\nabla}_{\hat{X}} f_1^{(0)} + N_{\text{Ca}1}^{-1} \langle \tilde{q}_{\text{total}1} \rangle_{\Omega_1} \cdot \vec{\nabla}_{\hat{Y}} f_1^{(1)} - \vec{\nabla}_{\hat{Y}} \cdot \Lambda_1^{(0)} \vec{\nabla}_{\hat{Y}} \frac{dP_{c1}}{df(S)} \Big|_{S^{(0)}} S^{(1)} = 0, \quad (16)$$

which can formally be solved with the method of Greens functions

$$S^{(1)} = -N_{\text{Ca}1}^{-1} \int G(\hat{Y}, \hat{Y}') \tilde{q}_{\text{total}1}(\hat{Y}') d\hat{Y}' \cdot \vec{\nabla}_{\hat{X}} f_1^{(0)}. \quad (17)$$

Considering the next order of the boundary flux

$$\left[ N_{\text{Ca}1}^{-1} \vec{q}_{\text{total}1} f_1^{(2)} - \Lambda_1^{(1)} \vec{\nabla}_{\hat{X}} P_{c1}^{(0)} - \Lambda_1^{(1)} \vec{\nabla}_{\hat{Y}} P_{c1}^{(1)} - \Lambda_1^{(0)} \vec{\nabla}_{\hat{Y}} P_{c1}^{(2)} - N_{g1} \Lambda_1^{(1)} \vec{e}_z \right] \cdot \vec{n} \Big|_{\Gamma_{12}} = \left[ -\Lambda_2^{(0)} \vec{\nabla}_{\hat{Y}} P_{c2}^{(0)} \right] \cdot \vec{n} \Big|_{\Gamma_{12}}, \quad (18)$$

we obtain the upscaled model by adding all terms of order  $\varepsilon^{-1}$  and  $\varepsilon^0$  and averaging spatially over the domain  $\Omega_1$  of the unit cell. The macroscopic variable of the problem is the saturation  $S_1^{(0)}$ , which depends only on the large scale variable  $\hat{X}$  and time  $t$ . It is

denoted in the following by  $S_m$ . Also, the gradient on the large scale  $\vec{\nabla}_X$  as macroscopic derivative is indicated by  $m$ .

$$\begin{aligned} \frac{\partial}{\partial t} S_m + \langle \vec{q}_{\text{total}1} \rangle_{\Omega_1} \cdot \vec{\nabla}_m f(S_m) - \vec{\nabla}_m \mathcal{D} \cdot \vec{\nabla}_m f(S_m) - \vec{\nabla}_m \frac{K_1}{\mu} \Lambda_1(S_m) \vec{\nabla}_m P_{c1} - \\ \vec{\nabla}_m \cdot \frac{K_1 \Delta \rho g}{\mu} \Lambda_1(S_m) \vec{e}_z = \frac{\partial}{\partial t} \langle S_2 \rangle_{\Omega_2}. \end{aligned} \quad (19)$$

Via the boundary flux we obtain here a coupling to the inclusion, which is driven by capillary forces. The highest order of the continuity equation in  $\Omega_2$  (order  $\varepsilon^{-2}$ ) reads

$$\frac{\partial}{\partial t} S_2 - \vec{\nabla}_{\hat{Y}} \Lambda_2^{(0)} \vec{\nabla}_{\hat{Y}} P_{c2}^{(0)}. \quad (20)$$

This means, the upscaled problem is coupled to small scale time dependent cell problems. They have to be solved for the (time dependent) boundary condition

$$P_{c1}|_{\Gamma_{12}} = P_{c2}|_{\Gamma_{12}} \quad (21)$$

on the interface between stagnant and mobile zones  $\Gamma_{12}$ .

The shape of the upscaled model resembles, for example, upscaled solute transport models with diffusive exchange with stagnant zones. Similar to these models, the memory term might be parameterized to make the model local in time.

## REFERENCES

- [1] Heiss, V.I., I. Neuweiler and A. Färber, The influence of the heterogeneous structure on the spatially averaged fluid distribution during immiscible displacement, Proceedings of the IAHR International Groundwater Symposium Istanbul, (2008).
- [2] Hornung, U., *Homogenization and Porous Media*, Springer, (1997).
- [3] Langlo, P. and M. S. Espedal, Macrodispersion for two-phase, immiscible flow in porous media, *Advances in Water Resources*, 17, 297-316, (1995).
- [4] Lewandowska, J., A. Szymkiewicz, K. Burzynski and M. Vauclin, Modeling of unsaturated water flow in double-porosity soils by the homogenization approach, *Advances in Water Resources*, 27, 283-296, (2004).
- [5] Neuweiler, I., S. Attinger, W. Kinzelbach and P.R. King: Large scale mixing for immiscible displacement in heterogeneous porous media, *Transport in Porous Media* 51, 287-314, (2003).
- [6] Noetinger, B., P. E. Spesivtsev, and E. V. Teodorovich, Stochastic analysis of a displacement front in a randomly heterogeneous medium, *Fluid dynamics*, 41 (5), 830-842, (2006).